Field-effect modulation of transport properties of charge-ordered $La_{1/3}Sr_{2/3}FeO_3$ thin films

K. Ueno,[1,*] A. Ohtomo,[1,†] F. Sato,[2] and M. Kawasaki[1]
[1]*Institute for Materials Research, Tohoku University, Sendai 980-8577, Japan*
[2]*Institute of Multidisciplinary Research for Advanced Materials, Tohoku University, Sendai 980-8577, Japan*
(Received 3 November 2005; revised manuscript received 13 February 2006; published 5 April 2006)

Temperature dependencies of field-effect transfer characteristics and Hall-effect properties have been studied for $La_{1/3}Sr_{2/3}FeO_3$ epitaxial films, which exhibit abrupt metal-to-insulator transition identical to that of a bulk. The field-effect transistors were fabricated with a channel consisting of an epitaxial interface between the $La_{1/3}Sr_{2/3}FeO_3$ film and an insulating $SrTiO_3$ single crystal substrate with a gate electrode on the back side. They operated in the *p*-type accumulation mode both in the high-temperature metallic state and low-temperature charge-ordered state. Field-effect mobility showed a good agreement with Hall mobility in the high-temperature metallic state. In addition, the Hall mobility in the charge-ordered state was found to exhibit an anomalous minus (*n*-type) sign although that in the metallic state and the field-effect results at all temperatures exhibited normal (*p*-type) sign. The Hall coefficient in the charge-ordered state is thought to be dominated by an anomalous Hall effect, and field-effect measurements can give information of charge transport on such conditions.

DOI: 10.1103/PhysRevB.73.165103 PACS number(s): 85.30.Tv, 71.30.+h, 72.20.Fr, 73.40.Qv

I. INTRODUCTION

Fundamental studies of field-effect (FE) modulation on strongly correlated electron systems have been extensively studied in recent years. They have been mainly aimed at modulation of the critical temperatures of superconducting cuprates.[1] It has been also of great interest if one can control metal-to-insulator transition (MIT) accompanying various spatial ordering structures in degrees of freedom of electrons such as ferromagnetic or antiferromagnetic spin ordering, charge ordering (CO), and orbital ordering.[2–6] Such studies showed that external-electric field can induce a change in resistivity and such an electrostatic response gives information about the ordering structures.[3,6] Here, we use a field-effect transistor (FET) structure to study a CO phase in $La_{1/3}Sr_{2/3}FeO_3$ (LSFO) thin films. LSFO is known to show a CO (charge disproportionation) of Fe^{3+} and Fe^{5+} along the pseudocubic [111] direction below a critical temperature of $T_{CO} \sim 190$ K, while it has a partially-filled metallic band above T_{CO} (see the inset of Fig. 1 and Ref. 7). At the phase boundary between CO and metallic states, an abrupt change in resistivity was observed for a bulk,[7] and for a thin film.[8] Such a dramatic change in resistivity at MIT has been rarely reported in epitaxial thin films of other charge-ordered perovskites. In addition, detailed examination of the MIT in LSFO has been mainly studied by Mössbauer[9]and photoemission,[8,10] but little is known about particular transport properties, e.g., carrier mobility and Hall coefficient. These facts propel us to study this material as a model of charge-ordered perovskites.

In this paper, we report both on FE transfer characteristics and on Hall-effect properties simultaneously measured for LSFO films. We choose the insulating $SrTiO_3$ (STO) substrate as a gate insulator, since lattice mismatch between LSFO and STO is small and high dielectric constant of STO is ideal for the FE study. We have successfully modulated the charge density up to $\sim 1 \times 10^{19}$ cm^{-3} by reducing STO thickness to 50 μm and applying a gate voltage up to 400 V (80 kV/cm). A good agreement between Hall and FE mobilities in a metallic high-temperature phase manifests high-quality heterointerfaces of the device with low defect density. In addition, we find that the Hall coefficient in the charge-ordered low-temperature phase exhibits a sign anomaly, as opposed to the normal *p*-type sign obtained from the FE results. This discrepancy is discussed with regard to magnetotransport of LSFO with the charge ordering accompanying antiferromagnetic spin ordering.

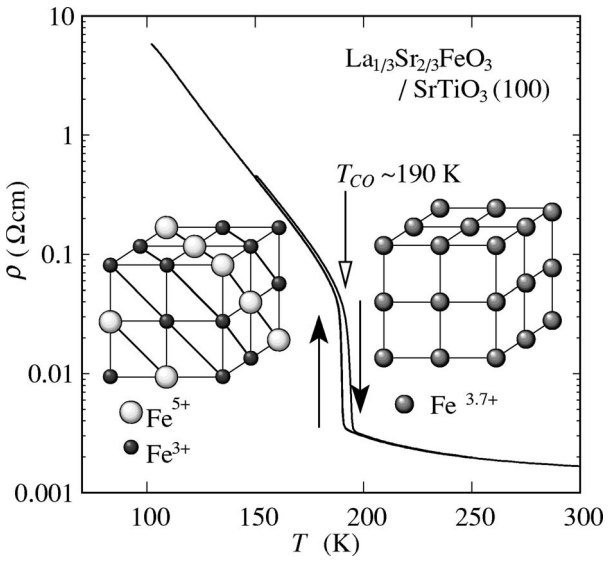

FIG. 1. Temperature dependence of the resistivity for a $La_{1/3}Sr_{2/3}FeO_3$ thin film. Arrows show resistivity hysteresis between the cooling and warming process. Inset shows schematics of the charge distribution in $La_{1/3}Sr_{2/3}FeO_3$ in a low-temperature insulating state (left) and high-temperature metallic state (right).

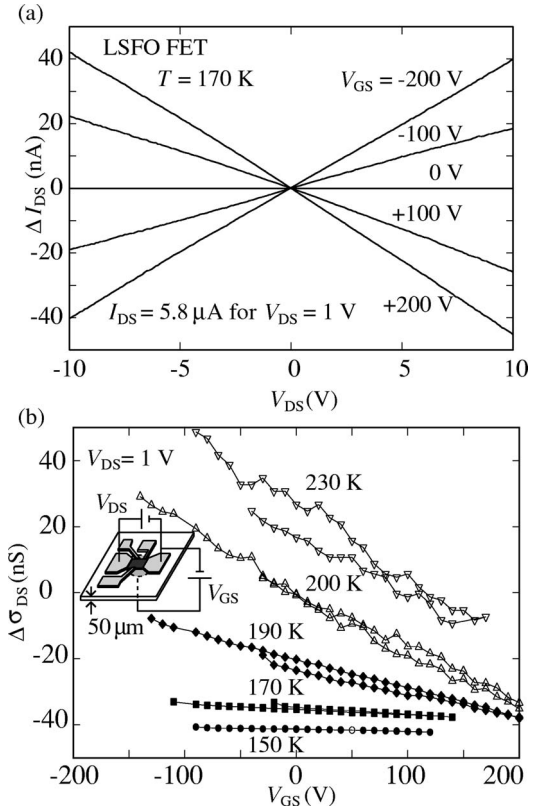

FIG. 2. (a) Difference in drain-source current ΔI_{DS} $[I_{DS}(V_{GS}) - I_{DS}(V_{GS}=0\ \mathrm{V})]$ plotted against the drain-source voltage V_{DS} for a $La_{1/3}Sr_{2/3}FeO_3/SrTiO_3$ FET at various gate voltages V_{GS}. (b) The V_{GS} dependence of channel conductivity modulation $\Delta\sigma_{DS}$ measured at $V_{DS}=1$ V at various temperatures. Inset depicts a schematic drawing of the device geometry and a measurement configuration.

II. EXPERIMENTS

The LSFO films were grown on (001) STO single crystalline substrates by the KrF excimer laser deposition in 10^{-3} Torr of oxygen at 1050 °C with typical fluence and repetition rate at 2 J/cm^2 and 1 Hz, respectively. The films were annealed at the growth condition for 1 h followed by another annealing in 1 atm of oxygen at 550 °C for 1 h. It should be mentioned that the high-temperature annealing is necessary to obtain a metallic low-resistivity film. The second annealing removes oxygen vacancies and transforms the crystalline structure from oxygen-vacancy ordered Brownmillerite to perovskite. The annealed films have tensile strain ($a=3.908$ Å and $c=3.865$ Å), indicating that a coherent perovskite lattice continues across the interface. The entire region of the channels shows an atomically flat surface with smooth terraces and steps of single unit-cell height.

The FETs based on the lattice-matched LSFO/STO heterostructures were fabricated with the gate electrodes directly formed on the backside of the substrates. The films with thickness D of 10 nm were patterned into Hall bars with channel length L and width W of 220 μm and 60 μm, respectively [see the inset of Fig. 2(b) and Ref. 11). The electrodes were 10 nm thick Ni film covered by 100 nm thick Au film, both of which were thermally evaporated. The surface of the film was coated by a photoresist for protection and the back of the substrate was mechanically polished to reduce the thickness to approximately 50 μm. After the photoresist was removed by acetone, the sample was annealed in 1 atm of oxygen at 550 °C for 1 h in the PLD chamber to remove the oxygen vacancy and surface defect, if any. Gold wires were attached on all of the electrodes and the back of the sample (i.e., gate electrode) by a conducting gold paint. It is noted that the thinned substrates showed identical permittivity to that of a pristine STO single crystal, namely, quantum paraelectric behavior at low temperatures. We used the obtained permittivity (e.g., $\epsilon_r=5.2\times10^2$ at $T=200$ K) for deducing the FE characteristics discussed below. The field-effect characteristics were measured using the Keithley 6517 electrometer and Agilent 4155C semiconductor parameter analyzer. Quantum Design PPMS was used to measure resistivities and magnetotransport properties.

III. RESULTS

The films exhibit MIT with an abrupt change in the resistivity by one order of magnitude as shown in Fig. 1. Thermal hysteresis appears as shown by upward and downward arrows, corresponding to resistivities obtained during cooling and warming the sample, respectively. The temperature dependence of the resistivity is virtually identical to that of a bulk single crystal.[7]

The device showed a typical p-type FET behavior in a temperature range including the MIT. Figure 2(a) shows the drain-source voltage (V_{DS}) dependencies of the change in drain-source current (ΔI_{DS}) at given gate voltages (-200 V $\leqslant V_{GS} \leqslant 200$ V) with respect to I_{DS} at $V_{GS}=0$. Application of negative bias induces accumulation of positive charges at the interface, resulting in the gain in channel conductivity ($\sigma_{DS}=I_{DS}/V_{DS}$). The σ_{DS} decreases when the positive gate bias is applied. These I_{DS}-V_{DS} curves were obtained in the insulating state, and similar characteristics appeared down to 150 K. The linear slope of the ΔI_{DS}-V_{DS} implies a linear region of operation and indicates good Ohmic contacts of the source and drain with the channel.

In order to examine V_{GS} dependence of conductivity modulation ($\Delta\sigma_{DS}=\Delta I_{DS}/V_{DS}$) shown in Fig. 2(b), we fixed V_{DS} at 1 V and scanned V_{GS} in a range where gate leakage current did not exceed 1 nA. The measurements were performed on different devices from the one used for Fig. 2(a). It is clearly seen that the $\Delta\sigma_{DS}$ linearly increases with decreasing V_{GS}, reflecting p-type channel characteristics. We note that the $\Delta\sigma_{DS}$-V_{GS} slope gradually increases as temperature increases. This is due to the temperature dependence of FE mobility as will be discussed later. It should be mentioned that we reproducibly observed similar p-type behavior both in metallic and insulating states for other several samples. Small hysteresis seen at $T \geqslant 190$ K arises from temperature drift during the V_{GS} scan at virtually fixed temperatures. Since the FE signal was too small in comparison to the I_{DS}, e.g., $\Delta I_{DS}/I_{DS} < 0.005$, even small temperature drift hampered the stable FE operation. Here, we note that the linear σ_{DS}-V_{GS} curve is also observed just above T_{CO} where

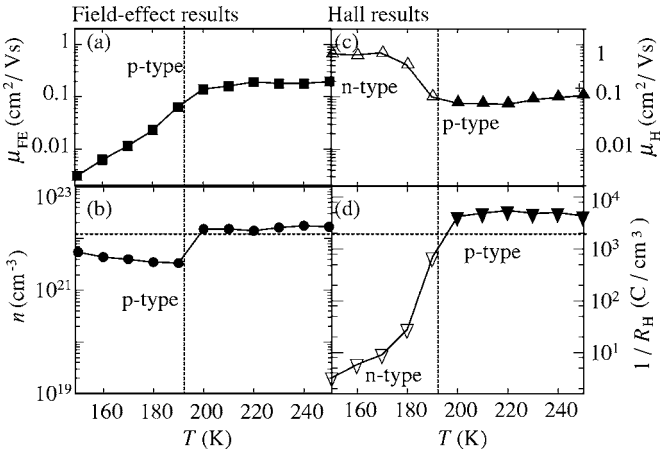

FIG. 3. (a) Temperature dependence of field-effect mobility μ_{FE} and (b) charge density n deduced from the resistivity and μ_{FE}. (c) Hall mobility μ_H and (d) inverse of Hall coefficient (R_H) as a function of temperature. Vertical broken lines denote the metal-insulator phase boundary. The $1/R_H$ on the right axis scales the charge density n on the left axis assuming that $n=1/(eR_H)$. Horizontal broken line denotes a charge density of 2/3 holes per Fe site, corresponding to the chemical formula of $La_{1/3}Sr_{2/3}FeO_3$.

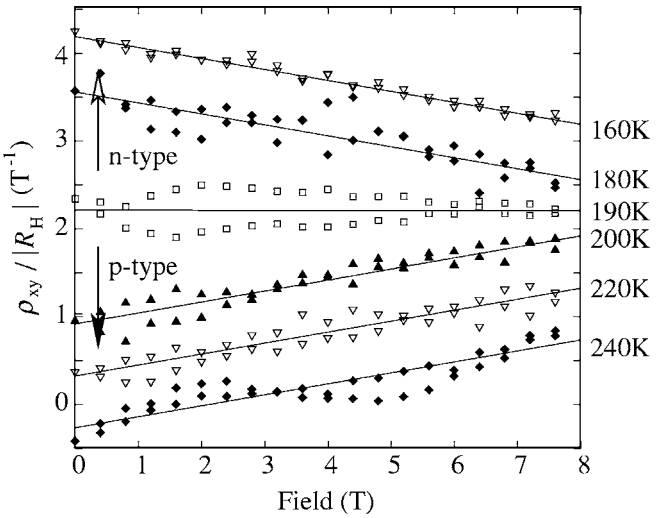

FIG. 4. The transverse resistivity ρ_{xy} divided by $|R_H|$ as a function of magnetic field. Solid lines are linear fits. Inversion in the sign of the Hall coefficient at the phase transition temperature ($T_{CO}\sim 190$ K) is clearly seen.

one may expect a dramatic FE response in the vicinity of the MIT.

From the results shown in Fig. 2(b), we examine the FE mobility μ_{FE} and charge density n at temperatures around MIT. The μ_{FE} was deduced using the general definition,

$$\mu_{FE} \equiv \frac{\partial I_{DS}}{\partial V_{GS}}\left(\frac{L}{C_i W V_{DS}}\right), \tag{1}$$

where C_i is a capacitance of the substrate per unit area. Assuming entire charges on the channel have an identical mobility equal to μ_{FE}, n is also defined as

$$n = \frac{\sigma}{\mu_{FE} e} = \frac{I_{DS}}{V_{DS}}\frac{L}{WD}\frac{1}{\mu_{FE} e}. \tag{2}$$

We plot the temperature dependence of μ_{FE} and n in the left panels of Fig. 3. In the insulating state, μ_{FE} gradually decreases with decreasing temperature. In contrast, in the metallic state, the μ_{FE} is almost independent of temperature. The value of n shows a discontinuity at MIT corresponding to the resistivity jump seen in Fig. 1.

We also carried out the Hall effect measurement for the same sample used for Fig. 2(b). The measured Hall voltages V_H depended both on a transverse Hall resistivity ρ_{xy} and on a longitudinal magneto-resistivity ρ_{xx} due to misalignment of Hall voltage probes. Since a ρ_{xy} is an odd function of magnetic field H and ρ_{xx} is an even function of H, we can estimate the ρ_{xy} from the measured V_H. Hall coefficient R_H was deduced from the slope of ρ_{xy}-H curves. We calculated the Hall mobility μ_H from a four-probe resistivity obtained for the same device. The right panels of Fig. 3 show the temperature dependence of R_H and μ_H. In the metallic state, both magnitude and sign of R_H agree with a hole concentration of 2/3 per Fe site expected from the chemical formula. Since R_H is nearly temperature-independent, transport properties of LSFO is similar to that of a highly doped (degenerated) semiconductor in the metallic state. Both temperature dependence and the magnitude of μ_H coincide with those of μ_{FE} in the metallic state. This fact clearly evidences that the heterointerface between the LSFO layer and the substrate are of high quality. If a FE device had an uncontrolled interface with many shallow traps, FE mobility would be much smaller than the drift mobility deduced by the Hall effect measurement.

Interestingly, the sign of R_H is opposite to what is expected for p-type materials below T_{CO} although p-type FET characteristics were observed at all temperatures. Figure 4 shows ρ_{xy} scaled by an absolute value of R_H plotted against the magnetic field at temperatures ranging from 150 K to 250 K. It is clearly seen that the slope of $\rho_{xy}/|R_H|$ inverts at T_{CO}. It is also noted that the value of R_H largely increases by more than two orders of magnitude as temperature goes down through T_{CO}. This is despite the fact that the resistivity increase at T_{CO} is only one order of magnitude. Consequently, μ_H at the insulating state results in about 10 times larger value than that of the metallic state.

IV. DISCUSSION

We now discuss the discrepancy between FE and Hall results, especially the inversion of the sign of the Hall coefficient and the increase of the Hall mobility towards the insulating state. In this system, charge ordering in the insulating state is known to cause an antiferromagnetic spin ordering along the ⟨111⟩ direction.[12] Therefore, the magnetic ordering is expected to cause the anomaly on the Hall coefficient. Indeed, NiO, which is an antiferromagnetic semiconductor, shows sign inversion on the Hall coefficient near the Neel temperature,[13] probably because magnetic ordering results in a large anomalous Hall coefficient with an opposite sign from the ordinary Hall coefficient.[14] Some of the metal-

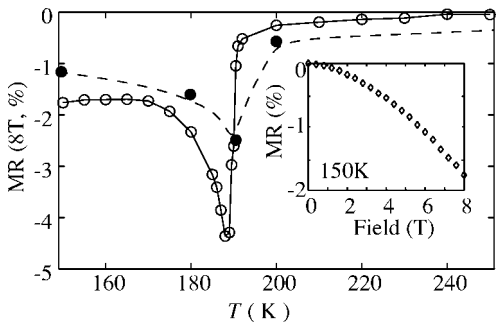

FIG. 5. Temperature dependence of magnetoresistance (MR) for a magnetic field of 8 T (open symbols). The magnetic field was applied perpendicular to the sample plane. Closed symbols and a broken line are refered from the Awana *et al.*'s results (Ref. 17). Inset shows the field dependence of magnetoresistance at 150 K.

lic ferromagnets, including perovskite oxides, $La_{1-x}Sr_xMnO_3$ (Ref. 15) and $Pr_{0.5}Sr_{0.5}MnO_3$,[16] also show a sign difference between anomalous and ordinary Hall coefficients, where the anomalous Hall contribution is distinguishable from an ordinary term due to their nonlinear field dependence of Hall resistivity. In our system, however, the anomalous Hall coefficient cannot be separated from the ordinary term because ρ_{xy}-H curves are linear up to 8 T. Therefore, we examined magnetoresistance (MR) in order to discuss how the magnetic ordering affects the charge transport. Awana *et al.* reported an abrupt increase of MR at T_{CO} for a polycrystalline sample of LSFO.[17] In our samples, the enhancement of MR was also observed, as shown in Fig. 5. Therefore, we think that interaction between the magnetic moments and the charges is enhanced when the charge disproportionation occurs. Anomalous Hall effect would be also enhanced by the charge ordering and antiferromagnetic spin ordering, and results in the anomaly on the Hall coefficient. It is noted that MR was not saturated even for a field of 8 T, as shown in the inset of Fig. 5. This coincides with the linear ρ_{xy}-H curves up to 8 T. In contrast, in the metallic state, the anomalous Hall effect was small enough and we can only observe the ordinary contribution of the Hall effect, which coincides with the field-effect measurement.

When the scattering process responsible for the anomalous Hall effect is not relevant to that for the longitudinal resistivity, $R_H(\sim\sigma_{xy}/\sigma_{xx}^2)$ would be proportional to ρ^2. In contrast, when a skew scattering of charge carriers by localized magnetic moment, R_H is proportional to ρ (Refs. 14 and 18). In our case, R_H is proportional to ρ below 170 K, i.e., $\mu_H(=R_H/\rho)$ is temperature independent. Therefore, the latter is thought to be more appropriate for LSFO. According to the calculation in an antiferromagnetic semiconductor,[14]

$$R_H = (1+\alpha)\frac{1}{ne}, \tag{3}$$

where α is a parameter determined by magnetic ordering structure and temperature. It is noted that, if we discuss the value and sign of n precisely, calculation of α is needed by using the magnetic structure of LSFO. Here, we only discuss the relative temperature dependence of n. Since both α and MR are dominated by magnetic scattering, we assume that α is a constant between 170 K and 150 K, where MR was temperature independent. Then, From Eq. (3) and Fig. 3(d), it is noticed that the carrier density n is exponentially decreased with decreasing temperature. Therefore, from the Hall results, we concluded that the charge disproportionation of LSFO results in a current conduction by a small number of charges, which are scattered by the localized charges with antiferromagnetically ordered spins.

However, from the FE results, the charge density was seen to be almost unchanged at the MIT and temperature independent in the insulating state. This is probably because the charge density obtained by the FE measurement is a total charge density at the Fermi surface, which includes both the conductive charges and localized charges on Fe^{3+} and Fe^{5+} ions. From a photoemission spectroscopy, the spectral weight on the Fermi surface was observed to be only gradually decreased with decreasing temperature,[10,19] and no large charge-ordered gap was observed. For example, the spectral weight at the Fermi surface at 170 K remains at about half of that at 210 K.[10] This observation supports the FE results. Therefore, combining the FE and Hall results, the increase of resistivity at the insulating state is concluded to not be due to a decrease of charge density at the Fermi surface, as expected from the Hall results, but due to a localization of charges at the Fermi surface.

V. CONCLUSION

We have successfully modulated charge concentration in LSFO thin films by applying an external electric field. The well-defined heterointerface between LSFO and STO was evidenced from a good agreement between the FE and the Hall coefficient in the metallic state. The Hall mobility in the insulating state has the anomalous minus (n-type) sign and is also temperature independent, both of which are different from the FE results. These discrepancies are considered to be due to a large anomalous Hall effect with an antiferromagnetic ordering of localized charges. Combining the FE and Hall examination, we can consistently explain how charges are localized in the LSFO. We conclude that the FE examination really gives information on the transport properties, which is not accessible by the Hall measurement alone. Thus we believe that the FE examination by using an epitaxial interface will be a useful method for studying the transport properties of other materials.

ACKNOWLEDGMENTS

We would like to thank to J. Nishimura, M. Ohtani, and T. I. Suzuki for technical help and valuable discussions. We also would like to thank J. Matsuno and H. Yamada for valuable discussions.

*Electronic address: uenok@imr.tohoku.ac.jp
†Also at: PRESTO, Japan Science and Technology Agency, Kawaguchi 332-0012, Japan.

[1] C. H. Ahn, J.-M. Triscone, and J. Mannhart, Nature (London) **424**, 1015 (2003).
[2] S. B. Ogale, V. Talyansky, C. H. Chen, R. Ramesh, R. L. Greene, and T. Venkatesan, Phys. Rev. Lett. **77**, 1159 (1996).
[3] T. Wu, S. B. Ogale, J. E. Garrison, B. Nagaraj, A. Biswas, Z. Chen, R. L. Greene, R. Ramesh, T. Venkatesan, and A. J. Millis, Phys. Rev. Lett. **86**, 5998 (2001).
[4] X. Hong, A. Posadas, A. Lin, and C. H. Ahn, Phys. Rev. B **68**, 134415 (2003).
[5] I. Pallecchi, L. Pellegrino, E. Bellingeri, A. S. Siri, and D. Marré, Phys. Rev. B **71**, 014406 (2005).
[6] M. Eblen-Zayas, A. Bhattacharya, N. E. Staley, A. L. Kobrinskii, and A. M. Goldman, Phys. Rev. Lett. **94**, 037204 (2005).
[7] T. Ishikawa, S. K. Park, T. Katsufuji, T. Arima, and Y. Tokura, Phys. Rev. B **58**, R13326 (1998).
[8] H. Wadati, D. Kobayashi, H. Kumigashira, K. Okazaki, T. Mizokawa, A. Fujimori, K. Horiba, M. Oshima, N. Hamada, M. Lippmaa, M. Kawasaki, and H. Koinuma, Phys. Rev. B **71**, 035108 (2005).
[9] T. Kawakami, S. Nasu, T. Sasaki, K. Kuzushita, S. Morimoto, S. Endo, T. Yamada, S. Kawasaki, and M. Takano, Phys. Rev. Lett. **88**, 037602 (2002).
[10] J. Matsuno, T. Mizokawa, A. Fujimori, K. Mamiya, Y. Takeda, S. Kawasaki, and M. Takano, Phys. Rev. B **60**, 4605 (1999).
[11] T. I. Suzuki, A. Ohtomo, A. Tsukazaki, F. Sato, J. Nishii, H. Ohno, and M. Kawasaki, Adv. Mater. (Weinheim, Ger.) **16**, 1887 (2004).
[12] P. D. Battle, T. C. Gibb, and P. Lightfoot, J. Solid State Chem. **84**, 271 (1990).
[13] H. J. van Daal and A. J. Bosman, Phys. Rev. **158**, 736 (1967).
[14] F. E. Maranzana, Phys. Rev. **160**, 421 (1967).
[15] A. Asamitsu and Y. Tokura, Phys. Rev. B **58**, 47 (1998).
[16] P. Wagner, D. Mazilu, L. Trappeniers, V. V. Moshchalkov, and Y. Bruynseraede, Phys. Rev. B **55**, R14721 (1997).
[17] V. P. S. Awana, J. Nakamura, J. Lindén, M. Karppinen, and H. Yamauchi, Solid State Commun. **119**, 159 (2001).
[18] J. Kondo, Prog. Theor. Phys. **27**, 772 (1962).
[19] H. Wadati, D. Kobayashi, A. Chikamatsu, R. Hashimoto, M. Takizaqwa, K. Horiba, H. Kumigashira, T. Mizokawa, A. Fujimori, M. Oshima, M. Lippmaa, M. Kawasaki, and H. Koinuma, J. Electron Spectrosc. Relat. Phenom. **144-147**, 877 (2005).